

In-phase and anti-phase flagellar synchronization by basal coupling

Gary S. Klindt,¹ Christian Ruloff,² Christian Wagner,^{2,3} and Benjamin M. Friedrich^{4,*}

¹Max Planck Institute for the Physics of Complex Systems, 01187 Dresden, Germany

²Experimental Physics, Saarland University, 66041 Saarbrücken, Germany

³Physics and Materials Science Research Unit, University of Luxembourg, 1511 Luxembourg, Luxembourg

⁴cfaed, TU Dresden, 01062 Dresden, Germany

(Dated: November 19, 2021)

We present a theory of flagellar synchronization in the green alga *Chlamydomonas*, using full treatment of flagellar hydrodynamics. We find that two recently proposed synchronization mechanisms, basal coupling and flagellar waveform compliance, stabilize anti-phase synchronization if operative in isolation. Their nonlinear superposition, however, stabilizes in-phase synchronization as observed in experiments. Our theory predicts different synchronization dynamics in fluids of increased viscosity or external flow, suggesting a non-invasive way to control synchronization by hydrodynamic coupling.

Keywords: cilia, flagella, synchronization, hydrodynamic interaction, low Reynolds number

Introduction. Pairs of coupled oscillators can synchronize with a fixed phase difference, a phenomenon first observed by Huygens for a pair of pendulum clocks [1]. Since then, synchronization has been described for many physical systems, including beating flagella [2], pairs of heart muscle cells [3], or light-driven micro-mills [4]. In each of these different systems, the dynamics towards a synchronized state is well approximated by the classic Adler equation for the phase difference δ between two weakly coupled oscillators [5, 6], which reads (for the simplest case of identical intrinsic frequencies $\omega_0 = 2\pi/T$ and absence of noise)

$$\dot{\delta} = -\frac{\lambda}{T} \sin \delta, \quad \delta_{\text{IP}}^* = 0, \quad \delta_{\text{AP}}^* = \pi. \quad (1)$$

The two steady states of Eq. (1), δ_{IP}^* and δ_{AP}^* , characterize in-phase synchronization (IP) and anti-phase synchronization (AP), respectively, see Fig. 1(a,b). The sign of the effective synchronization strength λ selects which state is stable. Unless the oscillator coupling possesses special symmetries, λ is generically non-zero [7, 8]. Its sign, however, depends on non-generic features of the system. For example, for a system of two beating metronomes on a moving tray – a modern day analogue of Huygens’ pendulum clocks – both IP and AP synchronization were observed, depending on subtle features like friction with the floor [9].

At the microscopic scale of biological cells, cilia and flagella represent a prime example of a chemo-mechanical oscillator. Molecular motors inside the flagellum drive regular bending waves of these slender cell appendages [10], rendering the flagellar beat a stable limit-cycle oscillator [11–13]. Pairs of flagella can synchronize their beat, e.g. in the green alga *Chlamydomonas* that swims with $n = 2$ flagella like a breast-stroke swimmer [14–16]. IP synchrony of its two flagella is a prerequisite for swimming straight and fast. The basal bodies of the two flagella are connected by a so-called distal striated fiber [17]. More complex flagellar gaits were observed

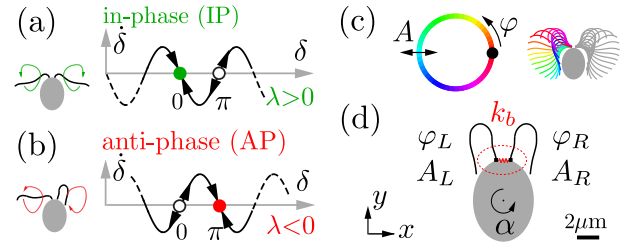


FIG. 1: In-phase and anti-phase synchronization. (a) The generic Adler equation, Eq. (1), predicts stable in-phase synchronization for a pair of coupled oscillators with phase difference $\delta = 0$ for synchronization strength $\lambda > 0$, corresponding to “breast-stroke swimming” *Chlamydomonas*. (b) For $\lambda < 0$, anti-phase synchronization is stable, corresponding to a “free-style gait” [18]. (c) In our theory, we characterize each flagellum as a limit-cycle oscillator with phase φ and amplitude A , which uniquely determine flagellar shapes [13]. (d) We consider a generic elastic coupling between flagella bases with stiffness k_b , see Eq. (6).

in species with $n = 2^k$ flagella, with matching patterns of basal coupling [18]. On epithelial surfaces, $n \gg 10^2$ flagella phase-lock their beat, thus forming metachronal waves [19], which facilitates efficient fluid transport [20–22]. Flagellar synchronization has been studied intensively in the model organism *Chlamydomonas*, reporting both IP and AP beating. While wild-type *Chlamydomonas* cells usually display IP synchrony, stochastic switching between regimes of stable IP and AP beating has been observed in a flagellar mutant (ptx1) [23]. Another mutant (vfl) with impaired basal coupling displayed lack of coordinated flagellar beating altogether [18, 24].

A long-standing hypothesis states that flagellar synchronization arises from a hydrodynamic coupling between flagella [25], as demonstrated for pairs of flagellated cells held at a distance [26]. A popular minimal model of this phenomenon abstracts from the specific shape of flagellar bending waves and represents each flag-

ellum by a sphere moving along a circular orbit [27–33]. The motion of the left and the right sphere with respective phase angles φ_L and φ_R is described by a balance of forces between active driving forces Q_j and hydrodynamic friction forces

$$Q_j = \Gamma_{jL}\dot{\varphi}_L + \Gamma_{jR}\dot{\varphi}_R, \quad j \in \{L, R\}. \quad (2)$$

Specifically, $\Gamma_{LL}\dot{\varphi}_L$ is the hydrodynamic friction force acting on the left sphere due to its own motion, and $\Gamma_{LR}\dot{\varphi}_R$ represents direct hydrodynamic interactions exerted by the right sphere on the left one. The minimal model possesses parity-time symmetry (PT), characterized by $\Gamma_{LR}(\varphi_L, \varphi_R) = \Gamma_{RL}(-\varphi_R, -\varphi_L)$, i.e. a spatial parity transformation ($\varphi_L \leftrightarrow -\varphi_R$) gives rise to an equivalent dynamics, but with time-arrow reversed [7, 8, 34]. Thus, there can be neither stable nor unstable states, unless PT-symmetry is broken.

A number of different PT-symmetry breaking effects have been proposed in the past, including interaction with boundary walls [27], phase-dependent driving forces $Q_j(\varphi)$ [29], and amplitude compliance with a variable radius $A(t)$ of each circular orbit, constrained by an elastic spring [28, 35]. In addition to direct hydrodynamic interactions between the two flagella, synchronization independent of hydrodynamic interactions can occur by a coupling between flagellar beating and the resultant motion of the cell [30]. Importantly, two recent experimental studies suggest that in *Chlamydomonas*, an elastic basal coupling connecting the proximal ends of both flagella could play a key role for flagellar synchronization [18, 24]. While each of these proposed mechanisms could in principle account for synchronization, it is not known, which symmetry breaking mechanism dominates in the real biological system. *A priori*, we do not even know if a specific mechanism will stabilize the IP or AP synchronized state.

Here, we theoretically study flagellar synchronization in the model organism *Chlamydomonas* to predict conditions for IP and AP synchrony, and present a first experiment to test our theory. We build on a previously developed description of the beating flagellum as a limit-cycle oscillator [13]. There, we retain the picture of a point moving along a circular orbit, yet each position of this point represents a genuine flagellar shape, see Fig. 1(c). Our theory uses detailed hydrodynamic calculations based on experimental beat patterns, to elucidate two PT-symmetry breaking effects: flagellar waveform compliance, and basal coupling between both flagella. We find that both PT-symmetry breaking mechanisms have a strong impact on synchronization, but only their combination yields IP synchrony with a synchronization strength sufficient to overcome noise [11, 15].

Effective theory of flagellar swimming and synchronization. Recently, we introduced an effective theory of flagellar swimming [13], there formulated for the case of synchronized beating only. The main idea behind

this theory is that regular flagellar bending waves represent a limit-cycle oscillator, which can be generically parametrized by a 2π -periodic phase variable φ obeying $\dot{\varphi} = \omega_0$ in the absence of an external perturbation, as well as a normalized amplitude A , which will always relax to a steady-state value A_0 . Any deviation from the reference condition, e.g. for asynchronous beating, external flow, or altered viscosity of the surrounding fluid, changes $\dot{\varphi}$ or A . We can thus describe the motion of a *Chlamydomonas* cell in a plane by a state vector \mathbf{q} comprising seven degrees of freedom, see Fig. 1(d)

$$\mathbf{q} = (\varphi_L, A_L, \varphi_R, A_R, \alpha, x, y)^T. \quad (3)$$

Here, φ_j, A_j with $j \in \{L, R\}$ denote phase and amplitude of the left and right flagellum, respectively, while α, x, y , denote orientation angle and center position of the cell body.

Each change of a degree of freedom will set the surrounding fluid in motion and induce hydrodynamic dissipation, in addition to friction inside the flagella. The total dissipation rate \mathcal{R} can be expressed in terms of generalized velocities \dot{q}_j and conjugated generalized friction forces P_j

$$\mathcal{R} = P_{\varphi_L}\dot{\varphi}_L + P_{A_L}\dot{A}_L + P_{\varphi_R}\dot{\varphi}_R + P_{A_R}\dot{A}_R + P_\alpha\dot{\alpha} + P_x\dot{x} + P_y\dot{y}. \quad (4)$$

The definition of the generalized friction forces P_j follows the framework of Lagrangian mechanics for dissipative systems, using \mathcal{R} as Rayleigh dissipation function [32, 36]. In the limit of zero Reynolds number, applicable to cellular self-propulsion where inertia is negligible [37], hydrodynamic friction forces are linear in the generalized velocities q_j , $P_i^{(h)} = \Gamma_{ij}^{(h)}\dot{q}_j$ (Einstein summation convention). The total friction forces $\mathbf{P} = \mathbf{P}^{(h)} + \mathbf{P}^{(i)}$ additionally comprise intraflagellar friction forces $\mathbf{P}^{(i)}$. For simplicity, we assume $P_i^{(i)} = \Gamma_{ij}^{(i)}\dot{q}_j$ with coefficients proportional to the respective hydrodynamic friction coefficients, i.e. $\Gamma_{ij}^{(i)} = (1 - \eta)/\eta \Gamma_{ij}^{(h)}$ for either $i, j \in \{\varphi_L, A_L\}$ or $i, j \in \{\varphi_R, A_R\}$ and $\Gamma_{ij}^{(i)} = 0$ else, where η denotes an energy efficiency of the flagellar beat.

We coarse-grain the activity of molecular motors inside each flagellum by active flagellar driving forces $Q_{\varphi_j}(\varphi_j)$ and amplitude restoring forces $Q_{A_j}(\varphi_j)$, $j \in \{L, R\}$. Thus, at each instance in time, we have 7 force balance equations

$$Q_j = P_j, \quad j \in \{\varphi_L, A_L, \varphi_R, A_R, \alpha, x, y\}. \quad (5)$$

Here, the generalized forces Q_x, Q_y , and Q_α represent constraining forces that ensure constraints of motion imposed on the cell. For a freely-swimming cell, force and torque balance imply $Q_x = Q_y = 0$, $Q_\alpha = 0$. For a fully clamped cell, one would impose $\dot{x} = 0$, $\dot{y} = 0$, $\dot{\alpha} = 0$, and determine the constraining forces Q_x, Q_y, Q_α such that the constraints are satisfied. With this

calibration, Eq. (5) fully specify equations of motions of flagellar swimming and synchronization.

Hydrodynamic computations allow us to determine all hydrodynamic friction coefficients $\Gamma_{ij}^{(h)}$ for a given flagellar beat pattern. Here, we use a fast boundary element method as described in [38] and a flagellar beat pattern recorded for the reference condition of a clamped cell with IP-synchronized beat [13]. There, the efficiency parameter has been estimated as $\eta = 0.21 \pm 0.06$ [13]. Additionally, the flagellar driving forces were uniquely calibrated from the requirement $\dot{\varphi}_L = \dot{\varphi}_R = \omega_0$ and $A_L = A_R = A_0$ for the reference case. The amplitude restoring forces Q_{A_j} determine how fast amplitude perturbations $A - A_0$ decay. Here, we assume exponential relaxation with a single relaxation time-scale τ_A for the reference condition, which uniquely determines Q_{A_j} [13]. For $\omega_0 \tau_A \ll 1$, perturbations cannot change the amplitude, while for $\omega_0 \tau_A \gg 1$ the limit cycle may become unstable. An analysis of amplitude fluctuations of the flagellar beat provided an estimate $\tau_A \approx 6$ ms [11]. We now use this theoretical description to predict dynamics after a perturbation of perfect synchrony for different PT-symmetry breaking scenarios.

Flagellar waveform compliance. Elastic degrees of freedom such as a flagellar waveform compliance can break PT symmetry in minimal models of hydrodynamically coupled oscillators, and thus allow for synchronization [28]. We tested this general proposition for the specific case of flagellar synchronization in *Chlamydomonas*, using our theoretical description with amplitude degrees of freedom A_L and A_R . We quantify the stability of the IP-synchronized state in terms of an effective synchronization strength λ , generalizing the parameter λ in Eq. (1), such that $-\lambda/T$ equals the cycle-average Ljapunov exponent for the phase difference $\delta = \varphi_L - \varphi_R$. The sign of λ indicates whether IP synchrony is stable ($\lambda > 0$) or not ($\lambda < 0$).

We computed λ for both the case of free-swimming and of clamped cells for two waveform data sets, see Fig. 2 and Fig. S4 in SM for $k_b = 0$ (no basal coupling). Whether a cell can swim freely, or is restrained from moving, can make a substantial difference for flagellar synchronization [16]. In the absence of flagellar waveform compliance ($\tau_A = 0$) and basal coupling ($k_b = 0$), we find $\lambda \approx 0.06$ for a free-swimming cell, and $\lambda \approx 0$ for a clamped cell, similar to a previous study [16] [42]. Amplitude compliance ($\tau_A > 0$) changes the synchronization strength, yet, surprisingly, destabilizes IP synchrony for free-swimming cells. Next, we study how an elastic basal coupling affects flagellar synchronization.

Basal body coupling. In *Chlamydomonas*, the proximal ends of both flagella are connected by a distal striated fiber, comprising an elastic basal coupling [17]. Previous experimental studies indicate the importance of this basal link for flagellar synchronization [18, 24]. In the following, we account for a finite elastic stiffness of

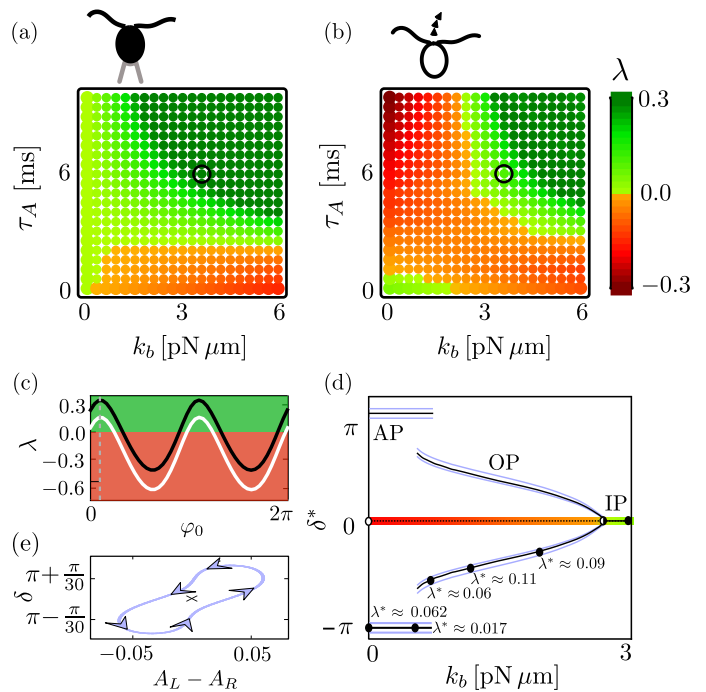


FIG. 2: Waveform compliance and basal coupling jointly determine synchronization dynamics in *Chlamydomonas*. (a) Computed synchronization strength λ (color code) as function of amplitude relaxation time τ_A and basal coupling stiffness k_b for a clamped cell. (b) Same for a free-swimming cell. (c) λ becomes maximal at $\varphi_0 \approx \pi/10$ for both clamped (black) and free-swimming cells (white). (d) Spontaneous symmetry breaking of synchronization: Cycle-averaged phase difference δ^* at steady state as function of basal stiffness k_B computed for a free-swimming cell (black). For selected steady states, we computed synchronization strengths λ^* characterizing Ljapunov exponents $-\lambda^*/T$ of convergence towards δ^* . Blue lines indicate maximum and minimum values of small-amplitude oscillations around δ^* at steady state, see also panel (e) [$k_b = 0$]. Parameters: $T = 20$ ms, $\tau_A = 6$ ms, $k_B = 3.6$ pN μ m, $\eta = 0.2$, $\mu = 0.85$ mPa s, $\varphi_0 = \pi/10$, unless stated otherwise.

this basal link, for which we assume a Hookian elastic energy

$$U_b = \frac{k_b}{2b_1^2} [b(\varphi_L, A_L, \varphi_R, A_R) - b_0]^2. \quad (6)$$

Here, $b(\varphi_L, A_L, \varphi_R, A_R)$ represent the elongation of the basal link, which is a periodic function of the two flagellar phases. In the absence of detailed knowledge of the elastic properties of the basal apparatus, we make the generic Ansatz $b(\varphi_L, A_L, \varphi_R, A_R) = b_0 + b_1 A_L \sin(\varphi_L - \varphi_0) + b_1 A_R \sin(\varphi_R - \varphi_0)$ with some phase shift φ_0 . The elastic energy of the basal link results in an additional term in the active flagellar driving force

$$Q_{\varphi_L} \rightarrow Q_{\varphi_L} - \frac{\partial U_b}{\partial \varphi_L |_{\varphi_L, A_L, \varphi_R, A_R}} + \frac{\partial U_b}{\partial \varphi_L |_{\varphi_L, A_L, \varphi_L, A_L}}, \quad (7)$$

and similarly for A_L , φ_R , A_R . Here, the last term merely reflects the fact that the elastic basal coupling must be incorporated in the calibration of the flagellar driving forces to yield $\dot{\varphi}_L = \dot{\varphi}_R = \omega_0$ in the reference case of IP-synchronized beating. Note that the unknown phase shift φ_0 affects synchronization, see Fig. 2(c).

Fig. 2(a,b) shows numerical results for the synchronization strength λ as a function of basal stiffness k_b for both clamped and free-swimming cells. Remarkably, basal coupling destabilizes IP synchrony in the absence of amplitude compliance, but stabilizes it for realistic values of the amplitude relaxation time τ_A and suitable choice of φ_0 . Thus, the combined effect of two PT-symmetry breaking mechanisms is opposite to the sum of their individual effects. A basal stiffness of $k_b = 3.6 \text{ pN } \mu\text{m}$ reproduces a previously measured value of $\lambda \approx 0.3$ for clamped cells [15]. With the length 300 nm and cross-sectional area $2 \cdot 10^4 \text{ nm}^2$ of the distal striated fiber [17], and assuming $b_1 = 50 \text{ nm}$, our estimate for k_b corresponds to a Young's modulus of approximately 20 kPa , well in the range of biological materials.

Out-of-phase synchronization. Flagellar synchronization by basal coupling exhibits dynamics that is more complex than the Adler equation. While we find stable AP and IP synchronization for sufficiently weak and strong basal coupling, respectively, consistent with Eq. (1), we find a regime of out-of-phase (OP) synchronization with $0 < \delta^* < \pi$ for intermediate coupling strengths, emerging from the IP-synchronized state by a pitchfork bifurcation, see Fig. 2(d). This OP synchronization represents an instance of spontaneous symmetry-breaking with two stable solutions $\pm\delta^*$.

Suggestions for experiments. Our theory suggests a non-invasive way to control flagellar synchronization. We predict that for external flow parallel to the long axis of a *Chlamydomonas* cell, the synchronization strength is reduced, see Fig. 3(a). Increasing the viscosity of the surrounding fluid gives similar results, see Fig. S6 in the Supporting Material (SM). Conceptually, imposing an external flow is equivalent to changing the phase-dependence of the flagellar driving forces, while increasing the viscosity reduces the magnitude of elastic coupling relative to viscous coupling.

We performed experiments, exposing *Chlamydomonas* cells held in micropipettes to external flow. We determined a flow-dependent synchronization strength $\lambda/(DT)$, normalized by an effective noise strength D of flagellar beating, see Fig. 3(b) and SM for details. Independent measurements reported $DT \approx 0.1 - 0.2$ [11, 39]. This suggests a quantitative match of theory and experiment.

Minimal model of synchronization by basal coupling. To gain insight into basic mechanisms of IP and AP synchronization, we revisit a popular minimal model of hydrodynamic synchronization [27–29]. Two spheres of equal radius r move inside a viscous fluid of viscosity μ

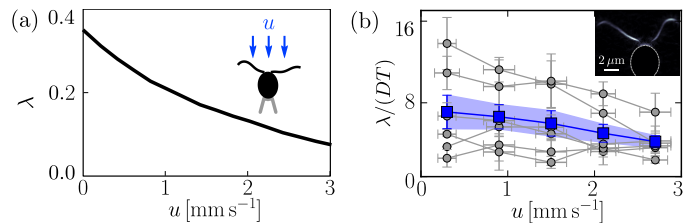


FIG. 3: Control of flagellar synchronization by external flow. (a) Theory: computed synchronization strength λ as function of external fluid flow with velocity u parallel to the long axis of the cell. (b) Experiment: measured synchronization strength $\lambda/(DT)$, normalized by effective noise strength D (blue: mean \pm s.e.m., $n = 6$ cells; gray: mean \pm s.e. for individual cells). Parameters: see Fig. 2.

along circular orbits \mathbf{r}_j of respective radii A_j , with centers separated by a distance d , $\mathbf{r}_j = A_j \mathbf{n}_j + \sigma_j d \mathbf{e}_x / 2$, for $j \in \{L, R\}$. Here, $\mathbf{n}_j = \cos \varphi_j \mathbf{e}_x + \sigma_j \sin \varphi_j \mathbf{e}_y$ denotes the radial vector and $\sigma_L = -1$, $\sigma_R = 1$. Each sphere is driven by a constant tangential driving force $Q_j = q_0$ with $q_0 = A_0^2 \gamma \omega_0$, friction coefficient $\gamma = 6\pi\mu r$ and reference amplitude A_0 . Hydrodynamic interactions couple the motion of both spheres. In the limit $r \ll d$ with A_0/r of order unity, $\Gamma_{LR} \dot{\varphi}_R = -A_L \gamma^2 \mathbf{t}_L \cdot \mathcal{G}(\mathbf{r}_L - \mathbf{r}_R) \cdot \dot{\mathbf{r}}_R$, and vice versa. Here, $\mathbf{t}_j = \partial \mathbf{n}_j / \partial \varphi_j$ is the tangent vector and $\mathcal{G}(\mathbf{r}) = (8\pi\mu)^{-1} [|\mathbf{r}|^{-1} + \mathbf{r} \otimes \mathbf{r} / |\mathbf{r}|^3]$ denotes the Oseen tensor. For constant amplitude, $A_i = A_0$, the system possesses PT-symmetry and no net synchronization occurs [7, 8, 27]. Introducing amplitude compliance, $\gamma \dot{A}_L = -k_A (A_L - A_0) - \gamma^2 \mathbf{n}_L \cdot \mathcal{G}(\mathbf{r}_R - \mathbf{r}_L) \cdot \dot{\mathbf{r}}_R$ with amplitude stiffness k_A for the left sphere and similarly for the right sphere, breaks PT-symmetry and results in $\lambda_a = -3\pi \tau_A \omega_0 r / (4d) + \mathcal{O}(r/d)^2$, where $\tau_A = \gamma / k_A$ denotes an amplitude relaxation time, see SM for details. Note that we consider counter-rotating spheres, mimicking a clamped *Chlamydomonas* cell [30, 31], while the originally studied case of co-rotating spheres yields $\lambda_a = 9\pi \tau_A \omega_0 r / (2d) + \mathcal{O}(r/d)^2$ [28]. Analogous to Eq. (7), we can introduce ‘basal coupling’ in this two-sphere model [with $U_b = k_b |\mathbf{r}_R - \mathbf{r}_L|^2 / (2A_0^2)$] as a second PT-symmetry breaking mechanism. This yields a synchronization strength $\lambda_b = -\pi k_b / q_0 + \mathcal{O}(r/d)$ in the absence of amplitude compliance with $\tau_A = 0$. Thus, both mechanisms imply $\lambda < 0$ for $r, A_0 \ll d$ if operative in isolation. Their nonlinear superposition, however, results in a positive cross-coupling term

$$\lambda = \lambda_a + \lambda_b + \frac{\pi}{2} (k_b / q_0)^2 \tau_a \omega_0 + \mathcal{O}(r/d). \quad (8)$$

As a consequence, IP synchrony is stable for suitable $k_b > 0$ and $\tau_A > 0$.

Discussion. Here, we presented a theory of flagellar swimming and synchronization for the model organism *Chlamydomonas*, to dissect the role of two proposed synchronization mechanisms, flagellar waveform compliance

[28] and elastic basal coupling [18, 24]. We find that each mechanism separately stabilized anti-phase synchronization in free-swimming cells, but their combination results in in-phase synchronization, as observed in experiments [14, 15].

Our theory makes specific predictions that can be tested in experiments. This includes altered synchronization dynamics in the presence of external flow or fluids of increased viscosity. Further, experimental disruption of the distal striated fiber that link the basal bodies of the two flagella, e.g. by laser ablation, could validate the role of basal coupling for synchronization proposed here. Interestingly, a change in length of the distal striated fiber, e.g. induced by intracellular calcium signaling [40], could allow the cell to switch between IP and AP synchronization (see Fig. S7 in SM), causing a ‘run-and-tumble’ motion as observed previously [41]. In conclusion, we have shown that synchronization strengths measured in experiments [15] cannot be explained in our theory without basal coupling, yet are reproduced for plausible parameter choices assuming such coupling.

Acknowledgment. G.S.K. and B.M.F. acknowledge support from the German Science Foundation “Microswimmers” Priority Program 1726 (Grant No. FR 3429/1-1).

* Electronic address: benjamin.m.friedrich@tu-dresden.de

- [1] A. Pikovsky, M. Rosenblum, and J. Kurths, *Synchronization* (Cambridge UP, 2001).
- [2] J. Gray, *Ciliary Movements* (Cambridge Univ. Press, Cambridge, 1928).
- [3] I. Nitsan, S. Drori, Y. E. Lewis, S. Cohen, and S. Tzlil, *Nat. Phys.* (2016).
- [4] J. Kotar, M. Leoni, B. Bassetti, M. C. Lagomarsino, and P. Cicuta, *Proc. Natl. Acad. Sci. U.S.A.* **107**, 7669 (2010).
- [5] R. Adler, *Proc. IRE* **34**, 351 (1946).
- [6] R. L. Stratonovich, *Topics in the Theory of Random Noise* (Gordon & Breach, 1963).
- [7] G. J. Elfring and E. Lauga, *Phys. Rev. Lett.* **103**, 088101 (2009).
- [8] B. M. Friedrich, *Eur. Phys. J. Spec. Top.* **225**, 2353 (2016).
- [9] J. Pantaleone, *Am. J. Phys.* **70**, 992 (2002).
- [10] B. Alberts, D. Bray, J. Lewis, M. Raff, K. Roberts, and J. D. Watson, *Molecular Biology of the Cell* (Garland Science, New York, 2002), 4th ed.
- [11] R. Ma, G. S. Klindt, I. H. Riedel-Kruse, F. Jülicher, and B. M. Friedrich, *Phys. Rev. Lett.* **113**, 048101 (2014).
- [12] K. Y. Wan, K. C. Leptos, and R. E. Goldstein, *J. R. Soc. Interface* **11**, 20131160 (2014).
- [13] G. S. Klindt, C. Ruloff, C. Wagner, and B. M. Friedrich, *Phys. Rev. Lett.* **117**, 258101 (2016).
- [14] U. Ruffer and W. Nultsch, *Cell Motil. Cytoskel.* **41**, 297 (1998).
- [15] R. E. Goldstein, M. Polin, and I. Tuval, *Phys. Rev. Lett.* **103**, 168103 (2009).
- [16] V. F. Geyer, F. Jülicher, J. Howard, and B. M. Friedrich, *Proc. Natl. Acad. Sci. U.S.A.* **110**, 18058 (2013).
- [17] D. L. Ringo, *Cell* **33**, 543 (1967).
- [18] K. Y. Wan and R. E. Goldstein, *Proc. Natl. Acad. Sci. U.S.A.* **113**, E2784 (2016), 1510.03272.
- [19] M. J. Sanderson and M. A. Sleight, *J. Cell Sci.* **47**, 331 (1981).
- [20] J. H. E. Cartwright, O. Piro, and I. Tuval, *Proc. Natl. Acad. Sci. U.S.A.* **101**, 7234 (2004).
- [21] N. Osterman and A. Vilfan, *Proc. Natl. Acad. Sci. U.S.A.* **108**, 15727 (2011).
- [22] J. Elgeti and G. Gompper, *Proc. Natl. Acad. Sci. U.S.A.* **110**, 4470 (2013).
- [23] K. C. Leptos, K. Y. Wan, M. Polin, I. Tuval, A. I. Pesci, and R. E. Goldstein, *Phys. Rev. Lett.* **111**, 158101 (2013).
- [24] G. Quaranta, M. E. Aubin-Tam, and D. Tam, *Phys. Rev. Lett.* **115**, 238101 (2015).
- [25] G. I. Taylor, *Proc. Roy. Soc. Lond. A* **209**, 447 (1951).
- [26] D. R. Brumley, K. Y. Wan, M. Polin, and R. E. Goldstein, *eLife* **3**, 5030732 (2014).
- [27] A. Vilfan and F. Jülicher, *Phys. Rev. Lett.* **96**, 58102 (2006).
- [28] T. Niedermayer, B. Eckhardt, and P. Lenz, *Chaos* **18**, 037128 (2008).
- [29] N. Uchida and R. Golestanian, *Phys. Rev. Lett.* **106**, 058104 (2011).
- [30] B. M. Friedrich and F. Jülicher, *Phys. Rev. Lett.* **109**, 138102 (2012).
- [31] R. R. Bennett and R. Golestanian, *Phys. Rev. Lett.* **110**, 148102 (2013).
- [32] K. Polotzek and B. M. Friedrich, *New J. Phys.* **15**, 045005 (2013).
- [33] Y. Izumida, H. Kori, and U. Seifert, *Phys. Rev. E* **94**, 052221 (2016), 1602.07116.
- [34] J. Elgeti, R. G. Winkler, and G. Gompper, *Rep. Prog. Phys.* **78**, 056601 (2015).
- [35] M. Reichert and H. Stark, *Eur. Phys. J. E* **17**, 493 (2005).
- [36] H. Goldstein, C. Poole, and J. Safko, *Classical Mechanics* (Addison-Wesley, Reading, MA, 2002), 3rd ed.
- [37] E. Lauga and T. R. Powers, *Rep. Prog. Phys.* **72**, 096601 (2009).
- [38] G. S. Klindt and B. M. Friedrich, *Phys. Rev. E* **92**, 063019 (2015).
- [39] R. E. Goldstein, M. Polin, and I. Tuval, *Phys. Rev. Lett.* **107**, 148103 (2011).
- [40] J. L. Salisbury and G. L. Floyd, *Science* **202**, 975 (1978).
- [41] M. Polin, I. Tuval, K. Drescher, J. P. Gollub, and R. E. Goldstein, *Science* **325**, 487 (2009).
- [42] There, $\eta = 1$, implying $\lambda \approx 0.3$, see Fig. S5 in SM.